


## Article

# Composite Polysilicate Metal Coagulants for Simultaneous Removal of Organic Matter, Phosphorus, and Ammonium-Nitrogen: Effects of Metal/Silicate Molar Ratio and Basicity

Hanxu Guo <sup>1</sup>, Peng Li <sup>2</sup>, Lianfeng Du <sup>2,\*</sup>, Guoyuan Zou <sup>2</sup> and Xuan Guo <sup>2,\*</sup> <sup>1</sup> School of Mechanical Engineering, Tiangong University, Tianjin 300387, China; hanxuguo2023@126.com<sup>2</sup> Institute of Plant Nutrition, Resources and Environment, Beijing Academy of Agriculture and Forestry Sciences, Beijing 100097, China

\* Correspondence: dulianfengyzs@163.com (L.D.); ytzxguoxuan@126.com (X.G.)

**Abstract:** Coagulation can effectively recover substances from wastewater; however, there is a lack of efficient coagulants for simultaneous recovery of organic matter, nitrogen, and phosphorus. We prepared a composite polysilicate metal (CSM) flocculant by combining  $\text{Fe}^{3+}$  and  $\text{Mg}^{2+}$  ions in polysilicic acid (PSiA). According to the results of scanning electron microscopy (SEM), X-ray diffraction (XRD), and Fourier-transform infrared spectroscopy (FTIR), the CSM exhibited a larger amorphous phase along with new compounds, including  $\text{Mg}_3\text{Fe}_2(\text{SiO}_4)_3$  and hydroxyl metals. The CSM demonstrated a higher coagulation efficiency than PSiA and polymeric ferric sulfate, particularly for  $\text{PO}_4^{3-}\text{-P}$  and  $\text{NH}_4^+\text{-N}$  removal. The metal/silicate molar ratio substantially influenced the structure and composition of the CSM, along with the coagulation efficiency, with an optimal ratio of 3:1. Additionally, we proposed a novel preparation strategy to achieve an optimum CSM basicity ( $B^*$ ) for coagulation by adjusting the initial pH of PSiA ( $\text{pH}_{\text{Initial}}$ ) without adding an alkali agent. The results demonstrated that the optimum  $B^*$  can be obtained by adjusting  $\text{pH}_{\text{Initial}}$  to 0.5 or 1. The overall optimum coagulation performance for the simultaneous removal of organic matter,  $\text{PO}_4^{3-}\text{-P}$ , and  $\text{NH}_4^+\text{-N}$  from wastewater was 68.5%, 99%, and 17.5%, respectively. This study provides a feasible approach for synchronous pollutant recovery from wastewater.

**Keywords:** coagulation; inorganic polymeric flocculants; ammonium-nitrogen recovery; basicity; domestic wastewater treatment



**Citation:** Guo, H.; Li, P.; Du, L.; Zou, G.; Guo, X. Composite Polysilicate Metal Coagulants for Simultaneous Removal of Organic Matter, Phosphorus, and Ammonium-Nitrogen: Effects of Metal/Silicate Molar Ratio and Basicity. *Water* **2023**, *15*, 1782. <https://doi.org/10.3390/w15091782>

Academic Editor: Alexandre T. Paulino

Received: 11 April 2023

Revised: 25 April 2023

Accepted: 5 May 2023

Published: 6 May 2023



**Copyright:** © 2023 by the authors. Licensee MDPI, Basel, Switzerland. This article is an open access article distributed under the terms and conditions of the Creative Commons Attribution (CC BY) license (<https://creativecommons.org/licenses/by/4.0/>).

## 1. Introduction

The recovery of organic matter, nitrogen, phosphorus, and other substances from wastewater is an important step in energy recovery and carbon neutralization in wastewater treatment [1,2]. Coagulation is an effective technology for direct pollutant removal from water. It is usually applied in drinking water treatment to remove particulate and colloidal substances from water [3]. Coagulation has also been broadly used in wastewater treatment to remove particulates, colloids, and phosphates [4,5]. Nevertheless, the removal and recovery of ammonium-nitrogen from wastewater by coagulation is currently limited; this hinders the synchronous recovery of organic matter, nitrogen, and phosphorus.

Coagulants are at the core of the coagulation process; those most predominantly used are aluminum or ferric salts, such as  $\text{AlCl}_3$  and  $\text{Fe}_2(\text{SO}_4)_3$  [4,6]. In recent decades, inorganic polymeric flocculants (usually abbreviated as IPFs), such as polyaluminium chloride (PAC) and polymeric ferric sulfate (PFS), have been developed [7,8]. Due to their sophisticated preparation procedures, they consist of effective coagulation species, and pre-polymerized IPFs are more effective than conventional simple inorganic salts [9,10]. Although IPFs exhibit better coagulation behavior than conventional inorganic salts, their bridge-aggregation ability is disrupted when compared to that of organic flocculants, such

as polyacrylamide (PAM) [11,12], because of their limited molecular size. To improve coagulation efficiency, other components, such as polysilicic acid (PSiA), have been introduced into IPFs [13,14], and are usually referred to as polysilicate metal coagulants. The primary purposes of introducing modifiers are to increase the molecular size, enhance the aggregation ability, and increase the stability and durability of the coagulant [15,16]. Compared to traditional coagulants, these demonstrate great advantages in the coagulation removal of pollutants in water, especially for particulate matter, colloids, and phosphate removal. However, the simultaneous removal of ammonium-nitrogen from water by these coagulants remains limited.

In recent years, magnesium precipitation has been widely used to achieve the simultaneous recovery of ammonium-nitrogen and phosphorus from water. Magnesium salt has been widely used to remove ammonium-nitrogen from wastewater, usually by dosing magnesium salt and  $\text{PO}_4^{3-}$  at a certain molar ratio under basic conditions to form undissolved struvite ( $\text{MgNH}_4\text{PO}_4 \cdot 6\text{H}_2\text{O}$ ) [17,18], and then removing ammonium-nitrogen through chemical precipitation. However, while this method is primarily used for chemical precipitation, few studies have combined struvite with coagulation to form coagulants with synchronous removal and recovery of organic matter, phosphate, and ammonium-nitrogen.

Basicity ( $B^*$ ) is an important index in IPFs and represents the degree of binding between metal ions and hydroxyl groups [19]. High basicity implies more effective components and better coagulation performance in the IPFs. In the preparation of IPFs, basicity is usually improved by adding alkalizing agents such as NaOH [20]. This undoubtedly increases the preparation costs of IPFs. Iron, aluminum, magnesium, and other metal ions can bind hydroxyl groups in water; this ability is related to the pH of the solution. By adjusting the pH of an aqueous solution, the ability of an IPF to capture hydroxyl groups, i.e., its basicity, can be achieved. To date, few studies have been conducted on the basicity adjustment of IPFs by adjusting the pH of the solution.

Therefore, in this study, we combined polysilicates with iron and introduced magnesium ions to prepare a composite polysilicate metal (CSM) coagulant. The structure and morphology of the samples were analyzed by scanning electron microscopy (SEM), X-ray diffraction (XRD), and Fourier-transform infrared spectroscopy (FTIR). The objectives of this study were: (i) to prepare a composite polysilicate metal coagulant and investigate its coagulation performance in wastewater; (ii) to evaluate two important impact factors, metal/silicate (M/Si) molar ratio and the initial pH of PSiA ( $\text{pH}_{\text{Initial}}$ ), on the characteristics and coagulation performance of CSM; and (iii) to investigate the potential of regulating the basicity of IPFs by adjusting  $\text{pH}_{\text{Initial}}$ . This study provides a feasible technology for the preparation of inorganic polymer coagulants and the simultaneous recovery of substances, especially organic matter, phosphorus, and ammonium-nitrogen, from wastewater.

## 2. Materials and Methods

### 2.1. Chemicals

$\text{Na}_2\text{SiO}_3 \cdot 9\text{H}_2\text{O}$ ,  $\text{MgSO}_4 \cdot 7\text{H}_2\text{O}$ ,  $\text{Fe}_2(\text{SO}_4)_3$ , and polymeric ferric sulfate (PFS) were procured from Sinopharm Chemical Reagent Company. All reagents were analytically pure chemicals, and deionized water was used to prepare the solutions.

### 2.2. Preparation of Composite Polysilicate Metal Coagulants

The CSMs were prepared by hydroxylation of a mixture of PSiA and metal salts ( $\text{Fe}^{3+}$  and  $\text{Mg}^{2+}$ ) using  $\text{Na}_2\text{SiO}_3 \cdot 9\text{H}_2\text{O}$ ,  $\text{Fe}_2(\text{SO}_4)_3$ , and  $\text{MgSO}_4 \cdot 7\text{H}_2\text{O}$  as raw materials.

#### 2.2.1. Metal/Silicate Molar Ratio Solutions

$\text{Na}_2\text{SiO}_3 \cdot 9\text{H}_2\text{O}$  was dissolved and diluted to obtain a PSiA solution at a concentration of 0.15 mol/L and  $\text{pH} = 4$ . As its viscosity increased to 0.005–0.006 Pa·s,  $\text{Fe}_2(\text{SO}_4)_3$  and  $\text{MgSO}_4$  with an Fe: Mg molar ratio of 1:1 were added to the solution under vigorous stirring to obtain the M/Si molar ratios of 2:1, 3:1, and 4:1. The mixture was stirred for 30 min

until it became transparent. It was then left to stand for 24 h, resulting in a homogeneous, transparent, and orange-yellow or orange-red solution.

### 2.2.2. $pH_{\text{Initial}}$ Solutions

To obtain CSM with different basicity values, a new strategy (see Section 2.5) was applied by adjusting the  $pH_{\text{Initial}}$  instead of adding extra alkalizing agents such as NaOH. The preparation procedure was similar to that described above, except that  $pH_{\text{Initial}}$  was adjusted to 0.5, 0.75, 1, 3, and 5. The M/Si molar ratio was 3:1.

### 2.3. Characterization of Composite Polysilicate Metal Coagulant

The liquid samples were vacuum-dried for 36 h at 60 °C in a DZF-6050 Vacuum Drying Oven (Lanphan, Shanghai, China) and then transferred to a desiccator at 25 °C. The solid products were pulverized for further characterization.

The morphologies of the coagulants were examined using a Hitachi S-4700 SEM. Crystalline phases were determined by XRD using a Siemens D-500 X-ray diffractometer (10–90°  $2\theta$  at 2°/min). Powdered coagulant was mixed with KBr and then analyzed by FTIR using a PerkinElmer spectrophotometer in the range of 400–4000  $\text{cm}^{-1}$ .

### 2.4. Coagulation Experiments

The wastewater used was real domestic wastewater obtained from the Beijing Academy of Agriculture and Forestry Sciences campus in Beijing, China. The main parameters were as follows: suspended solids (SS), 150–300 mg/L; chemical oxygen demand (COD), 350–500 mg/L;  $\text{PO}_4^{3-}\text{-P}$ , 3–5 mg/L;  $\text{NH}_4^+\text{-N}$ , 30–50 mg/L; temperature, 18–22 °C; pH, 6.5–7.5.

CSM, PSiA, and PFS were compared to determine their coagulation performance in domestic wastewater treatment. Coagulation tests were performed via a jar test apparatus with six paddles (MY3000-6B, Wuhan, China). Each wastewater sample (1.0 L) was transferred in a beaker and stirred rapidly at 150 rpm for 1.5 min after coagulant dosing (0–160 mg/L), followed by slow stirring at 80 rpm and 40 rpm for 5 min, and final sedimentation for 20 min. Supernatants were collected for SS, COD,  $\text{PO}_4^{3-}\text{-P}$ , and  $\text{NH}_4^+\text{-N}$  measurements. All analyses were performed according to the Standard Methods [21]. SS, COD,  $\text{PO}_4^{3-}\text{-P}$ , and  $\text{NH}_4^+\text{-N}$  were determined using gravimetric, potassium dichromate, potassium persulfate digestion-molybdenum antimony spectrophotometry, and Nessler's reagent spectrophotometry methods, respectively.

### 2.5. Relationship between $pH_{\text{Initial}}$ and Basicity

The evaluation of hydroxyl metals in IPFs is usually described by the basicity parameter ( $B^*$ , where  $B^* = [\text{OH}^-]/[\text{metal ions}]$ ), which has a substantial effect on the degree of polymerization and coagulation performance of IPFs. Tang and Stumm [22] suggested the following definition for Fe(III) solutions:

$$B^* = [\text{OH}^-]_{\text{bound}} / [\text{Fe}_T] = B_H + B - A \quad (1)$$

where  $[\text{OH}^-]_{\text{bound}}$  refers to the  $\text{OH}^-$  that participated in the polymerization.  $\text{Fe}_T$  is the total iron concentration.  $B_H$  is the initial ratio calculated from the pH of the initial solution.

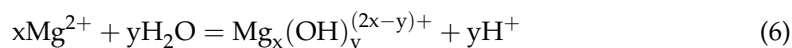
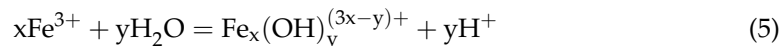
$$B_H = [\text{H}^+] / [\text{Fe}_T] = 10^{-\text{pH}} / [\text{Fe}_T] \quad (2)$$

$B$  and  $A$  are the added base and acid ratios,

$$B = [\text{OH}^-]_{\text{add}} / [\text{Fe}_T] \quad (3)$$

$$A = [\text{H}^+]_{\text{add}} / [\text{Fe}_T] \quad (4)$$

During the preparation of the CSM, solid metal salts were added directly to the PSiA solution, with no pre-hydrolysis of the metal ions. However, the pH of the solution decreased after the addition of metal salts, which was caused by binding of the added metal ions to the  $\text{OH}^-$  in the solution. After the metal salts are added, hydrolysis reactions occur as follows:



As shown in the equations above, when one unit of  $\text{OH}^-$  is grasped by the metal salts, one unit of  $\text{H}^+$  is produced, that is, the quantity of  $\text{OH}^-$  grasped by the metal salts equals that of  $\text{H}^+$  produced simultaneously. We evaluate the  $\text{OH}^-$  grasped by metal ions without the assist of added base by evaluating the alteration of pH values before and after the solid metals adding. Equation (1) can be modified as:

$$B^* = [\text{OH}^-]_{\text{bound}} / [M_T] = B_{H2} - B_{H1} + B - A \quad (7)$$

where  $M_T$  is the total metal concentration in CSM (mol/L),  $B_{H1}$  equates to  $B_H$  in Equation (1), and  $B_{H2}$  is the final ratio calculated from the pH value of the final solution. Thus, the basicity of CSM can be calculated as:

$$B^* = [10^{-\text{pH}_{\text{Final}}} - 10^{-\text{pH}_{\text{Initial}}} + C_B - C_A] / [M_T] \quad (8)$$

where  $C_B$  and  $C_A$  represent the concentrations of base and acid, respectively,  $\text{pH}_{\text{Initial}}$  is the initial pH value of PSiA, that is, pH value of PSiA in preparation, and  $\text{pH}_{\text{Final}}$  is the final pH value of the coagulant.

Equations (8) and (9) can be applied to the preparation of IPFs without metal pre-hydrolysis. When no extra base or acid is added during coagulant preparation, as applied in this study, Equation (9) is as follows:

$$B^* = [10^{-\text{pH}_{\text{Final}}} - 10^{-\text{pH}_{\text{Initial}}}] / [M_T] \quad (9)$$

## 2.6. Statistical Analysis

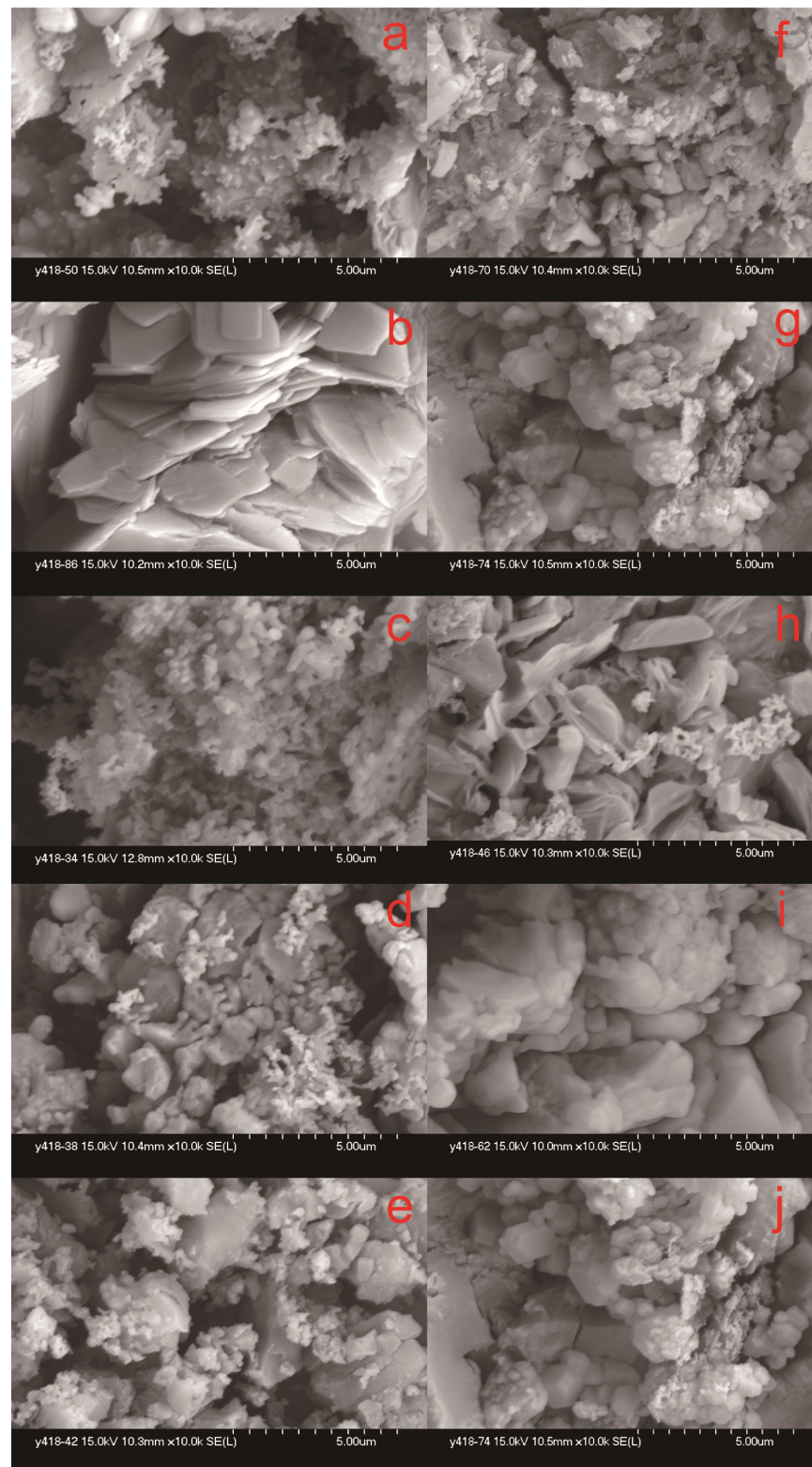
Statistical differences among the samples were evaluated using SPSS Statistics ver. 21.0 software, and  $p < 0.05$  was considered statistically significant. All assays were performed in duplicate, and data of all three replicates were subjected to an analysis of variance.

## 3. Results and Discussion

### 3.1. Morphology of Composite Polysilicate Metal Coagulant

Variations in the morphology of the CSM with different M/Si ratios were analyzed via SEM micrographs. As illustrated in Figure 1, CSM with small M/Si ratios consists of many tiny particles aggregated together, similar to those contained in PSiA (Figure 1a). As the M/Si molar ratio increased (Figure 1c–f), the CSM tended to exhibit a lump morphology. The lumps were unevenly distributed on the surface, indicating the presence of an amorphous phase. The major structures of the CSM were absorbed by tiny particles, which adhered to the major structure through aggregation, and their amount decreased as the M/Si molar ratio increased. This could be an evaluation of the aggregating ability of the CSM, suggesting that the aggregating ability decreases with decreasing silicate proportion.





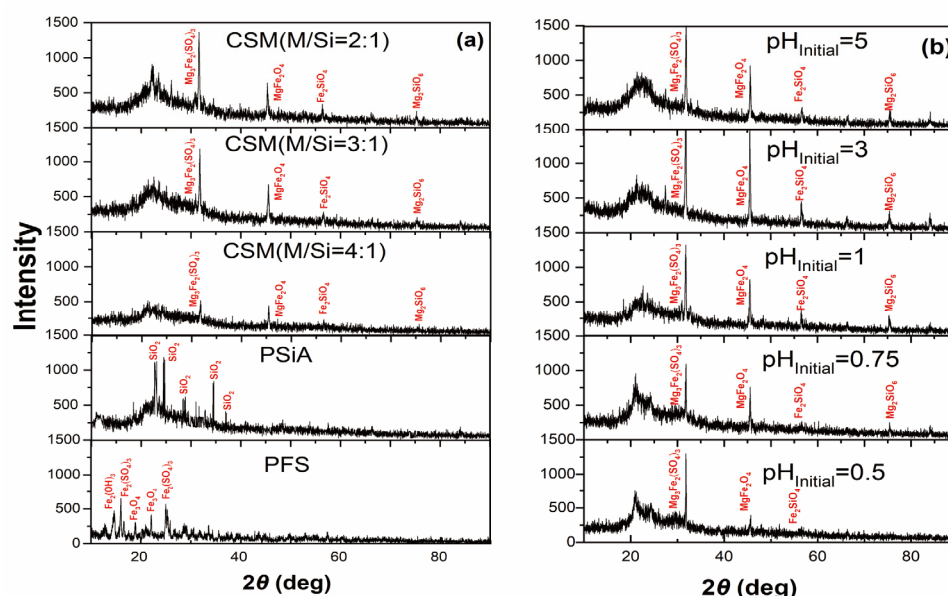
**Figure 1.** SEM spectra of PSiA, PFS and CSM: (a) PSiA; (b) PFS; (c) CSM (M/Si = 2:1); (d) CSM (M/Si = 3:1); (e) CSM (M/Si = 4:1); (f)  $\text{pH}_{\text{Initial}} = 0.5$ ; (g)  $\text{pH}_{\text{Initial}} = 0.75$ ; (h)  $\text{pH}_{\text{Initial}} = 1$ ; (i)  $\text{pH}_{\text{Initial}} = 3$ ; (j)  $\text{pH}_{\text{Initial}} = 5$ .

Figure 1f–j show SEM micrographs of the CSM at different  $\text{pH}_{\text{Initial}}$ . Generally,  $\text{pH}_{\text{Initial}}$  significantly affects the structure of the CSM. When  $\text{pH}_{\text{Initial}}$  was below one, the CSM had a predominantly sliced or lumped morphology. As  $\text{pH}_{\text{Initial}}$  increased to five, this structure

was rarely observed; however, some axiological or acicular particles aggregated. In addition, many tiny particles were adsorbed on the major structure when  $\text{pH}_{\text{Initial}}$  was below one; however, they disappeared when  $\text{pH}_{\text{Initial}}$  reached seven, similar to the analysis of the M/Si molar ratios, indicating a decrease in the aggregation ability of CSM.

### 3.2. XRD Analysis

Figure 2 shows the XRD patterns of the powdered PSiA, PFS, and CSM. In general, the CSM demonstrated a larger amorphous phase. Different from the XRD spectra of PSiA (Figure 2a), a large, broad peak was found at approximately  $2\theta = 20^\circ$ , indicating that the introduction of PSiA to metal salts possibly led to the amorphous phase of CSM. Additionally, the diffractive crystal spectra of  $\text{Fe}_2(\text{SO}_4)_3$ ,  $\text{Fe}(\text{OH})_3$ ,  $\text{Fe}_3\text{O}_4$ , and  $\text{SiO}_2$  disappeared, whereas several new compounds, including  $\text{Fe}_2\text{SiO}_4$ ,  $\text{Mg}_2(\text{SiO}_6)$ , and  $\text{MgFe}_2\text{O}_4$ , were observed. This indicates that Fe-Si, Mg-Si, Fe-O-Si, and Mg-O-Si bonds were formed, and that the CSM contained new species rather than a mixture of raw materials. Despite the XRD spectra of CSM with different M/Si molar ratios (Figure 2a) being similar, the intensity of the broad peak at approximately  $2\theta = 20^\circ$  decreased with increased M/Si molar ratios, suggesting that a higher proportion of metal favors less influence of polysilicate on CSM.



**Figure 2.** XRD spectra of CSM, PSiA and PFS: (a) PSiA, PFS and CSM with different M/Si molar ratios; (b) CSM with different  $\text{pH}_{\text{Initial}}$ , M/Si = 3:1.

The XRD spectra of the CSM with different  $\text{pH}_{\text{Initial}}$  (Figure 2b) were similar, and two large broad peaks were present. One was at around  $2\theta = 20^\circ$ , and another was at around  $2\theta = 30^\circ$ . As  $\text{pH}_{\text{Initial}}$  increased, the peak at approximately  $2\theta = 20^\circ$  tended to be sharp, intense, and crystallized compared to PSiA. This suggests that a lower  $\text{pH}_{\text{Initial}}$  resulted in lower degree of PSiA polymerization.

The peak at around  $2\theta = 30^\circ$  tended to be broad, intense, and bigger as  $\text{pH}_{\text{Initial}}$  decreased. The compounds involved with the peak at around  $2\theta = 30^\circ$  consisted predominantly of new compounds formed by Mg, Fe, and Si, such as  $\text{Mg}_3\text{Fe}_2(\text{SiO}_4)_3$ , suggesting that a lower  $\text{pH}_{\text{Initial}}$  favored the formation of Fe-Si, Mg-Si, or Fe-O-Si, Mg-O-Si bonds. New compounds, such as  $\text{Mg}_3\text{Fe}_2(\text{SiO}_4)_3$ , were formed by the metal ions and Si in the CSM.

### 3.3. FTIR Spectra Analysis

Figure 3a shows the FTIR spectra of CSM with M/Si molar ratios of 2:1, 3:1, and 4:1. CSM exhibited two characteristic bonds at  $3423\text{--}3400\text{ cm}^{-1}$  and  $1643\text{--}1635\text{ cm}^{-1}$ ; these are attributed to the vibration of -OH associated with metal ions [23,24]. The intensities of

both peaks increased as the M/Si molar ratio increased from 2:1 to 3:1 but decreased as the M/Si molar ratio increased further. This indicates that a metal proportion that is too small or too large leads to worse absorption, polymerization, and crystallinity of water during CSM coagulation.

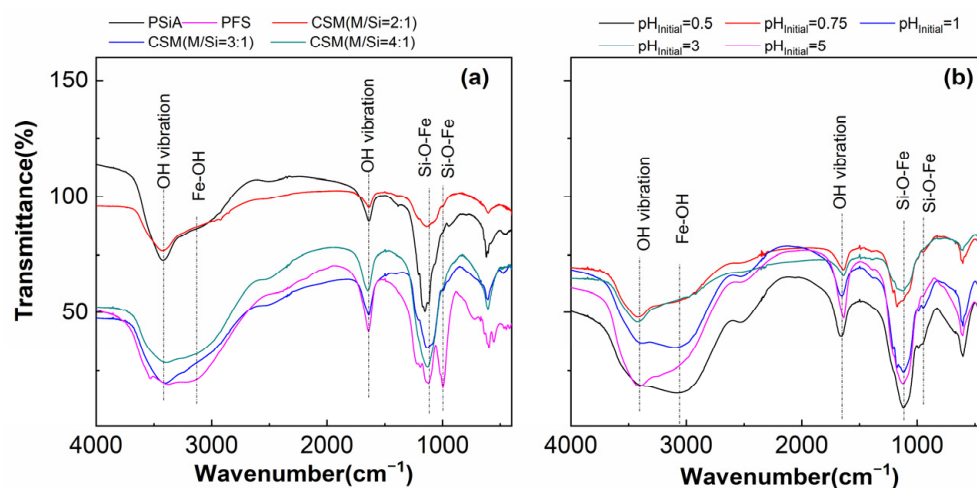


**Figure 3.** FTIR spectra of PSiA, PFS and CSM: (a) CSM with different M/Si molar ratios; (b) CSM with different  $pH_{Initial}$ , M/Si molar ratio = 3:1.

Strong absorption peaks were observed at 3000–2974  $cm^{-1}$ , corresponding to the vibration of Fe-OH [25–27]. The two peaks at 950–948  $cm^{-1}$  and 470  $cm^{-1}$  were associated with the Si-O-Fe and Si-O-Mg bonds, respectively [28]. When the M/Si molar ratio increased (Figure 3a), the peaks at 3000–2974  $cm^{-1}$  predominately increased, whereas the peaks at 950–948  $cm^{-1}$  and 470  $cm^{-1}$  decreased, indicating that the metal-O-Si bonds tended to transform into metal-OH bonds, i.e., hydroxyl magnesium and hydroxyl iron [29,30]. However, excess metal-OH bonds may lead to the formation of  $Fe(OH)_3$  and  $Mg(OH)_2$ , which cannot be dissolved in solution, thus reducing the effectiveness of CSM. An appropriate M/Si molar ratio should be determined to favor the formation of hydroxyl metals and avoid the formation of precipitates.

As the M/Si molar ratio decreased, the peaks at 1152–1122  $cm^{-1}$  and 950–948  $cm^{-1}$ , which corresponded with the O-Si and Si-O-metal bonds, respectively, increased [29,30]. This suggests that the introduction of PSiA favored the metal ions and that PSiA reacted together to form complex compounds consisting of both metal ions and PSiA. As the PSiA proportion increased, more metal ions tended to participate in the complexation, preventing the polymerization of silicate (to form Si-O-metal bonds); thus, the polymerization degree of CSM tended to be greater. It has been reported that a low silicate proportion favors the Si-O-metal-O-metal-Si bonds forming, whereas high silicate proportions favored forming Si-O-metal-Si-O-Si bonds [28,31].

The  $pH_{Initial}$  also substantially affected the FTIR spectra of the CSM (Figure 3b). When  $pH_{Initial}$  decreased, the peaks at 3000–2974  $cm^{-1}$  increased, whereas the peaks at 3423–3400  $cm^{-1}$  decreased, indicating that the dissociative -OH bond was probably transformed into a metal-OH bond. This suggests that a lower  $pH_{Initial}$  favors the formation of hydroxyl metals, which are effective components of CSM. The peaks at 2520–2514  $cm^{-1}$  increased with  $pH_{Initial}$ , which were related to the O-Fe and O-Mg bonds, indicating that a lower  $pH_{Initial}$  favored the formation of O-metal bonds.

### 3.4. Composite Polysilicate-Metal Coagulant Performance

The coagulation efficiency of CSM for treating domestic wastewater was evaluated by measuring removal efficiencies, including SS, COD,  $PO_4^{3-}$ -P, and  $NH_4^+$ -N, and compared to that of conventional coagulants (PSiA, and PFS).

### 3.4.1. Influence of Metal/Silicate Molar Ratios

Figure 4 presents the coagulation performance of domestic wastewater using CSM with different M/Si molar ratios. The coagulation performance was significantly influenced by the CSM dosage ( $p < 0.05$ ). At lower dosages, the coagulation performance was markedly improved with an increase in the CSM dosage; the optimal dosage of CSM was 60–80 mg/L, under which the removal efficiencies of SS, COD,  $\text{PO}_4^{3-}\text{-P}$ , and  $\text{NH}_4^+\text{-N}$  reached 98%, 65%, 99%, and 15%, respectively. These removal efficiencies were higher than PSiA and PFS ( $p < 0.05$ ), especially for  $\text{PO}_4^{3-}\text{-P}$  and  $\text{NH}_4^+\text{-N}$  removal. In addition, CSM exhibited significantly higher removal efficiencies of SS, COD,  $\text{PO}_4^{3-}\text{-P}$ , and  $\text{NH}_4^+\text{-N}$  than traditional coagulants ( $\text{FeCl}_3$  and  $\text{Al}_2(\text{SO}_4)_3$ ) at the same dosage (Table S1,  $p < 0.05$ ). The concentrations of SS, COD,  $\text{PO}_4^{3-}\text{-P}$ , and  $\text{NH}_4^+\text{-N}$  under optimal removal were 4 mg/L, 126 mg/L, 0.15 mg/L, and 21.9 mg/L, respectively. The coagulation process for hydrolyzing metals is a combination of charge neutralization, bridge aggregation, entrapment, and other reactions [32,33]. During the coagulation process, CSM can be hydrolyzed into polynuclear species of hydroxyl coordination compounds carrying a high positive charge, which exhibit a strong charge-neutralization reaction with suspended and colloidal particles, as well as negatively charged phosphate radicals with a negative charge. Meanwhile, the introduction of PSiA made the molar size and weight of CSM markedly larger than those of PFS, such that the polymeric species predominated in the coagulant, resulting in a higher coagulation efficiency. The adsorption of multinuclear and polymeric materials on the particles enables the formation of condensation bridges between adjacent particles, thus facilitating the subsequent formation of precipitation-prone flocculants [28,29,31,34]. Additionally, the dissociated  $\text{Mg}^{2+}$  and its hydrolyzed product  $\text{Mg}(\text{OH})^+$  can complex with  $\text{NH}_4^+\text{-N}$  in domestic wastewater, forming a precipitate  $\text{MgNH}_4\text{PO}_4$ , which is then absorbed by destabilizing particles.

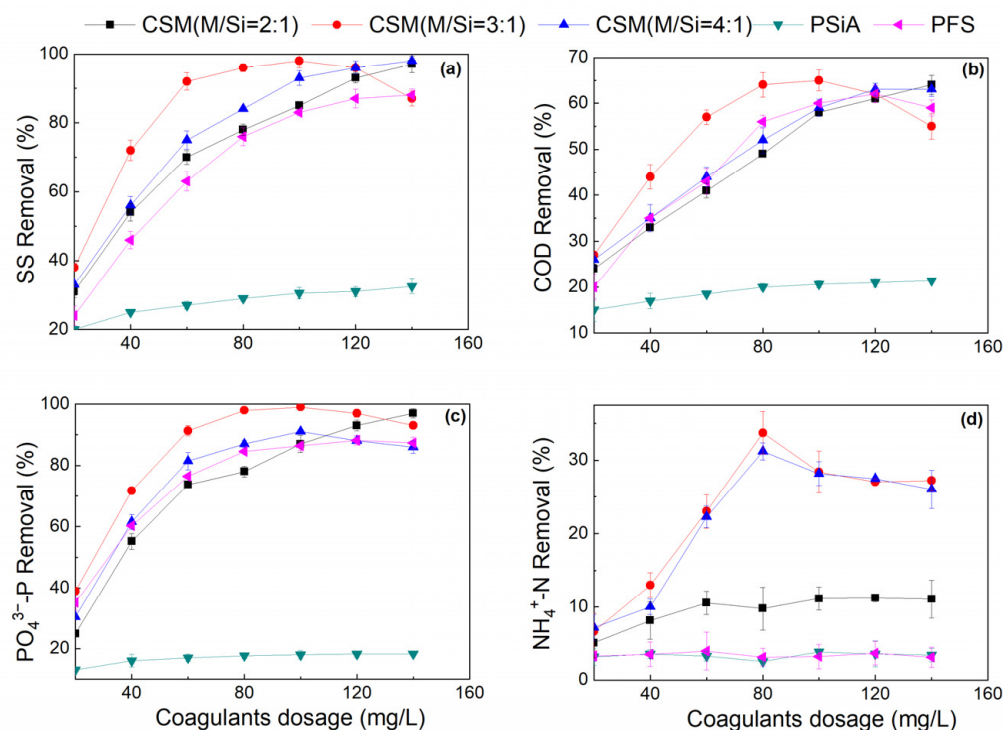


**Figure 4.** Coagulation efficiency of CSM ( $\text{pH}_1 = 2$ ) with different M/Si molar ratios treating domestic wastewater: (a) SS; (b) COD; (c)  $\text{PO}_4^{3-}\text{-P}$ ; (d)  $\text{NH}_4^+\text{-N}$ .

Additionally, an increase in the M/Si molar ratio led to a slight deterioration in the coagulation efficiency (Figure 4). This may be related to the reversal of the surface charge due to the excessive absorption of metal ions to the surface of the initial flocs, which could



hinder subsequent absorption, resulting in the failure to form large flocs [26]. As shown in Table S2, CSM with M/Si = 4:1 showed smaller floc size than that of CSM with M/Si = 3:1 at the end of coagulation process. The M/Si molar ratio represents the proportion of metal salts and silicate in the CSM, which are associated with the charge-neutralization capacity and bridge-aggregating ability, respectively [35]. A higher M/Si molar ratio indicates a greater charge-neutralization ability of CSM, whereas a lower M/Si molar ratio indicates a better bridge-aggregating capacity of CSM. Suspended and colloidal particles in domestic wastewater mainly carry negative charges, so that the M/Si molar ratio could facilitate charge neutralization to be destabilized by impurities. However, the particle surface charge reverses as the M/Si molar ratio continues to increase, unable to favor the formation of large flocs (Table S2), which has a similar mechanism as the coagulant dosage. Despite that, the floc size of CSM was significantly larger than those of PSiA and PFS (Table S2,  $p < 0.05$ ), resulting in higher coagulation performances of CSM.

### 3.4.2. Influence of Basicity and $\text{pH}_{\text{Initial}}$

The  $B^*$  parameter of CSM was calculated using Equation (9).  $B^*$  varied along with  $\text{pH}_{\text{Initial}}$  and had values of 0.08–1.29 (Table 1 and Figure 5a). When  $\text{pH}_{\text{Initial}}$  was 0–1, the  $B^*$  of CSM increased to a maximum of 1.29 at  $\text{pH}_{\text{Initial}} = 0.75$ , and then decreased as  $\text{pH}_{\text{Initial}}$  increased. The quantity of  $\text{OH}^-$  grasped by the metal ions can be attributed to two factors: the degree of dissociation of the metal ions and the concentration of  $\text{H}^+$  [36]. A higher degree of dissociation indicates a higher grasping ability; it could be very difficult for metal ions to grasp  $\text{OH}^-$  with a high concentration of  $\text{H}^+$ . When the  $\text{pH}_{\text{Initial}}$  was below 4, the metal ions mostly existed in a dissociated state, and the degree of dissociation increased with decreasing pH, which also indicated the higher grasping ability of the metal ions. However, a lower  $\text{pH}_{\text{Initial}}$  means a higher concentration of  $\text{H}^+$ , which competes with metal ions to grasp  $\text{OH}^-$ , resulting in a decrease in the  $B^*$  value of the CSM.

**Table 1.** Composite polysilicate metal (CSM) with different basicities ( $B^*$ ).

NO.	1	2	3	4	5	6	7	8	9
$\text{pH}_{\text{Initial}}$	0.25	0.50	0.75	1	2	3	4	5	6.00
$\text{pH}_{\text{Final}}$	0.15	0.26	0.30	0.48	1.02	1.24	1.33	1.55	1.68
$[\text{M}_\text{T}]$ (mol/L)	0.25	0.25	0.25	0.25	0.25	0.25	0.25	0.25	0.25
$B^*$	0.58	0.93	1.29	0.86	0.34	0.23	0.19	0.11	0.08

It has been reported that the  $B^*$  of IPFs can affect coagulation performance; generally, coagulants with larger  $B^*$  exhibit better coagulation efficiency [19]. Figure 5b shows the coagulation performance of domestic wastewater using the CSM with different  $B^*$ . The increase in  $B^*$  favored higher coagulation efficiency, and the optimum value was  $B^* = 1.0$ , when  $\text{pH}_{\text{Initial}} = 0.5$  or 1.0. Removal efficiencies of SS and COD were 99% and 68.5%, and 99% and 17.5%, respectively. However, an excessively large  $B^*$  can weaken the coagulation efficiency, probably because of excessive  $\text{OH}^-$  which may react with metal ions to form  $\text{Fe}(\text{OH})_3$  and  $\text{Mg}(\text{OH})_2$  precipitates. The relationship between the coagulation performance of the CSM and basicity was evaluated (Figure 5b). A good correlation between the coagulation performance of the CSM and their basicities was found ( $R^2 > 0.8$ ), which meant that a larger  $B^*$  would enhance the coagulation performance of the CSM.

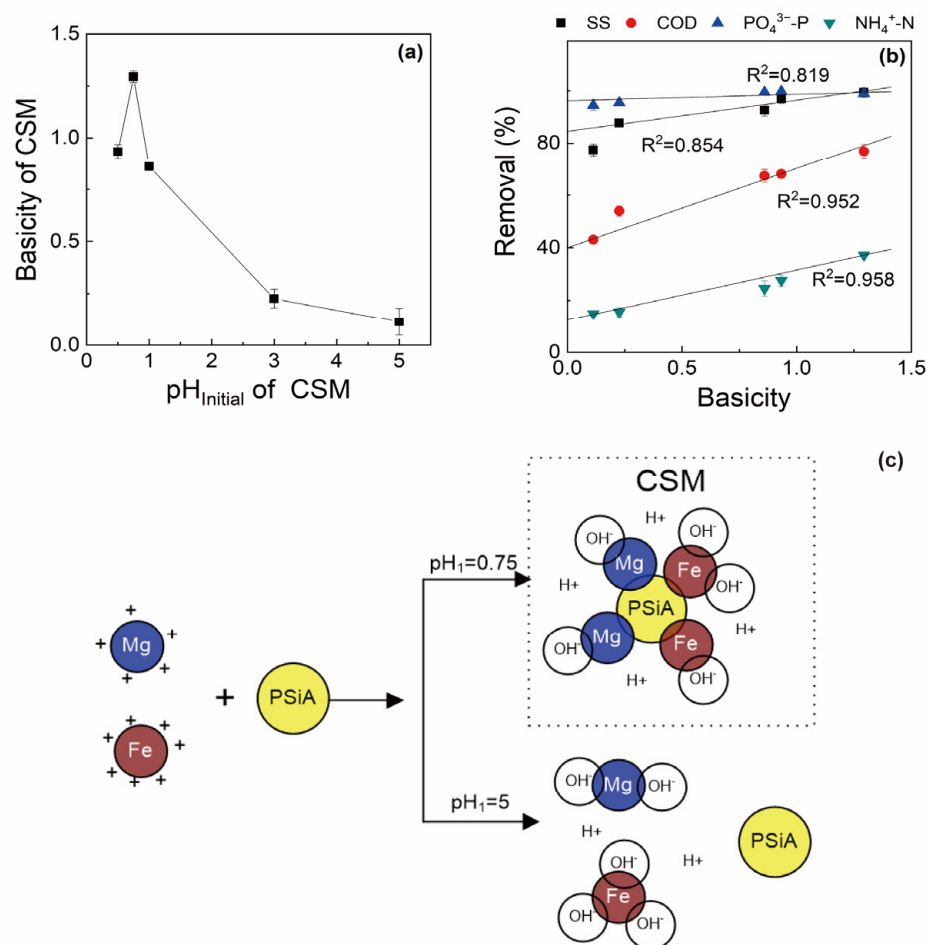


**Figure 5.** Basicity (a) and coagulation efficiency (b) of CSM (M/Si molar ratio = 3:1) with different basicities treating domestic wastewater. (c) shows the potential mechanism of basicity adjustment by  $pH_{Initial}$ .

Here, the purpose of adjusting the  $pH_{Initial}$  was to make the solution acidic before polymerization, under which the metal ions were dissociated; this is so that metal ions such as  $Fe^{3+}$  and  $Mg^{2+}$  could have a strong ability to grasp  $OH^-$  in the coexisting solution, aiming to form hydroxyl metals, which are the prerequisite and efficient constituents of CSM (Figure 5c). The quantity of  $OH^-$  grasped by the metal ions can be attributed to two factors: the degree of dissociation of the metal ions and the concentration of  $H^+$ . A higher degree of dissociation indicates a higher grasping ability; it could be very difficult for metal ions to grasp  $OH^-$  with a high concentration of  $H^+$ . When the solution pH was 4, Fe and Mg mainly existed in dissociated states ( $Fe^{3+}$  and  $Mg^{2+}$ ) [22], and the degree of dissociation increased with decreasing pH, which also indicated a higher grasping ability for metal ions. However, a solution with a very low pH ( $<0.75$ ) indicates a higher concentration of  $H^+$ , which would compete with metal ions to grasp  $OH^-$ , resulting in a decrease in the  $B^*$  of CSM. In contrast, when the pH was above four, Fe and Mg mainly existed as metal-hydroxyl complexes, such as  $Fe(OH)_3$  and  $Mg(OH)_2$  (Figure 5c), which were mainly precipitated in which Fe and Mg were not dissociated; thus, they could not grasp  $OH^-$  to form larger metal-Si-O complexes during the secondary preparation of CSM. Therefore,  $pH_{Initial}$  played a predominant role in the preparation of CSM, and the optimum value was 0.5 or 1, at which point the  $B^*$  of CSM could reach 1.29. Additionally, this preparation method does not require supplemental basic chemicals, such as NaOH or  $NaHCO_3$ , but requires the adjustment of  $pH_1$  to obtain the optimum basicity of coagulants, when compared with traditional methods for preparing inorganic polymer flocculants [7,14,30]. Compared with

traditional methods, this could be an efficient way to reduce costs. However, the  $B^*$  value of CSM in this study was still lower than that of the other IPF prepared by adding an additional alkalizing agent. Future studies should focus on improving the  $B^*$  without using an additional alkalizing agent. In addition, the introduction of Mg into CSM greatly enhanced the removal of  $\text{NH}_4^+\text{-N}$  from wastewater, resulting in the simultaneous removal of organic matter, phosphorus, and ammonium-nitrogen. This method provides a feasible approach for the simultaneous recovery of various pollutants from wastewater.

#### 4. Conclusions

A composite polysilicate metal (CSM) coagulant was prepared to enhance the removal of pollutants from wastewater. The M/Si molar ratio and  $B^*$  significantly affected the structure and composition of CSM. XRD and FTIR analyses suggest that CSM presents a larger amorphous phase, and that Fe-Si, Mg-Si, Fe-O-Si, Mg-O-Si, and metal-OH bonds are formed. New compounds such as  $\text{Mg}_3\text{Fe}_2(\text{SiO}_4)_3$  were formed by metal ions and Si in the CSM. CSM exhibited significantly better coagulation efficiency than PSiA and PFS, especially for  $\text{PO}_4^{3-}\text{-P}$  and  $\text{NH}_4^+\text{-N}$  removal in domestic wastewater treatment. The coagulation efficiency increased with dosage and M/Si molar ratio, with optimum values of 60–80 mg/L and 3:1, respectively. A novel strategy to obtain the basicity ( $B^*$ ) of CSM was achieved by adjusting the PSiA  $\text{pH}_{\text{Initial}}$ , which was calculated using the method proposed in this paper. The optimum  $B^*$  of the CSM for domestic wastewater treatment was approximately 1.0, when  $\text{pH}_{\text{Initial}} = 0.5$  or 1.0. Future studies should focus on improving the  $B^*$  without using an additional alkalizing agent.

**Supplementary Materials:** The following supporting information can be downloaded at: <https://www.mdpi.com/article/10.3390/w15091782/s1>, Table S1: Comparison of coagulation performance between CSM and traditional coagulants ( $\text{FeCl}_3$  and  $\text{Al}_2(\text{SO}_4)_3$ ) at the same dosage (80 mg/L); Table S2: Floc size of different coagulants at the end of coagulation processes.

**Author Contributions:** Conceptualization, X.G.; Data curation, X.G.; Funding acquisition, L.D., G.Z. and X.G.; Investigation, X.G.; Project administration, G.Z.; Resources, L.D.; Supervision, P.L., L.D. and G.Z.; Validation, H.G., P.L., G.Z. and X.G.; Writing—original draft, H.G. and X.G. All authors have read and agreed to the published version of the manuscript.

**Funding:** This work was supported by projects provided by the Key R&D Plan of China [2021YFD1700500], Beijing Academy of Agriculture and Forestry Sciences [YZS202101, KJCX20220408, ZHS202303], and the Young Talent Support Project from CAST [YESS20200159].

**Data Availability Statement:** Data will be available due to request.

**Conflicts of Interest:** The authors declare no conflict of interest. The funders had no role in the design of the study; in the collection, analyses, or interpretation of data; in the writing of the manuscript; or in the decision to publish the results.

#### References

- Li, W.W.; Yu, H.Q.; Rittmann, B.E. Chemistry: Reuse water pollutants. *Nature* **2015**, *528*, 29–31. [CrossRef]
- Du, W.J.; Lu, J.-Y.; Hu, Y.-R.; Xiao, J.; Yang, C.; Wu, J.; Huang, B.; Cui, S.; Wang, Y.; Li, W.-W. Spatiotemporal pattern of greenhouse gas emissions in China's wastewater sector and pathways towards carbon neutrality. *Nat. Water* **2023**, *1*, 166–175. [CrossRef]
- Malkoske, T.A.; Berube, P.R.; Andrews, R.C. Coagulation/flocculation prior to low pressure membranes in drinking water treatment: A review. *Environ. Sci. Water Res. Technol.* **2020**, *6*, 2993–3023. [CrossRef]
- Abujazar, M.S.S.; Karaagac, S.U.; Abu Amr, S.S.; Alazaiza, M.Y.D.; Bashir, M.J.K. Recent advancement in the application of hybrid coagulants in coagulation-flocculation of wastewater: A review. *J. Clean. Prod.* **2022**, *345*, 131133. [CrossRef]
- Zhao, C.; Zhou, J.; Yan, Y.; Yang, L.; Xing, G.; Li, H.; Wu, P.; Wang, M.; Zheng, H. Application of coagulation/flocculation in oily wastewater treatment: A review. *Sci. Total Environ.* **2021**, *765*, 142795. [CrossRef] [PubMed]
- Ang, W.L.; Mohammad, A.W. State of the art and sustainability of natural coagulants in water and wastewater treatment. *J. Clean. Prod.* **2020**, *262*, 121267. [CrossRef]
- Li, L.; Piao, Y.; Ma, F.; Sheng, T.; Sun, C.; Liu, W. Preparation of a novel inorganic-biological composite flocculant for the removal of turbidity and organic matter in the surface water. *Desalin. Water Treat.* **2020**, *180*, 219–226. [CrossRef]
- Yu, L.; Liu, P.; Zheng, K. Preparation of polymeric ferric sulfate -quaternary ammonium cationic-modified starch composite flocculant and its application in oily sludge treatment. *Environ. Prot. Eng.* **2022**, *48*, 35–49. [CrossRef]

9. Guo, Y.; Li, X.; Sun, J.; Liu, Y.; Wang, H.; Ding, J.; Chen, L.; Tian, X.; Yuan, Y. Physicochemical characterization and flocculation performance evaluation of PAC/PMAPTAC composite flocculant. *J. Appl. Polym. Sci.* **2022**, *139*, 51653. [\[CrossRef\]](#)
10. Lee, K.E.; Morad, N.; Teng, T.T.; Poh, B.T. Development, characterization and the application of hybrid materials in coagulation/flocculation of wastewater: A review. *Chem. Eng. J.* **2012**, *203*, 370–386. [\[CrossRef\]](#)
11. Deng, X.; Zhao, J.; Qiu, X.; Duan, Y.; Ren, X.; Li, W.; Mu, R.; Yuan, H. Magnesium Hydroxide Slurry Coagulation-Adsorption Performance for Reactive Orange Removal Assisted with PAM. *Water Air Soil Pollut.* **2023**, *234*, 176. [\[CrossRef\]](#)
12. Qin, J.; Wang, H.; Qin, C.; Meng, H.; Qu, W.; Qian, H. The role of sodium carbonate in PAM coagulation-flocculation for oil acidized wastewater treatment. *Water Sci. Technol.* **2018**, *77*, 2677–2686. [\[CrossRef\]](#) [\[PubMed\]](#)
13. Hu, P.; Su, K.; Sun, Y.; Li, P.; Cai, J.; Yang, H. Efficient removal of nano- and micro- sized plastics using a starch-based coagulant in conjunction with polysilicic acid. *Sci. Total Environ.* **2022**, *850*, 157829. [\[CrossRef\]](#) [\[PubMed\]](#)
14. Wei, Y.; Ding, A.; Luo, F.; Li, N.; Yao, C. Comparison of polysilicic acid (PSiA) and magnesium sulfate modified polysilicic acid (PMSiS) for effective removal of Congo red from simulated wastewater. *Korean J. Chem. Eng.* **2020**, *37*, 978–984. [\[CrossRef\]](#)
15. Deng, B.; Luo, H.; Jiang, Z.; Jiang, Z.-J.; Liu, M. Co-polymerization of polysilicic-zirconium with enhanced coagulation properties for water purification. *Sep. Purif. Technol.* **2018**, *200*, 59–67. [\[CrossRef\]](#)
16. Tang, Y.; Hu, X.; Cai, J.; Xi, Z.; Yang, H. An enhanced coagulation using a starch-based coagulant assisted by polysilicic acid in treating simulated and real surface water. *Chemosphere* **2020**, *259*, 127464. [\[CrossRef\]](#)
17. Tansel, B.; Lunn, G.; Monje, O. Struvite formation and decomposition characteristics for ammonia and phosphorus recovery: A review of magnesium-ammonia-phosphate interactions. *Chemosphere* **2018**, *194*, 504–514. [\[CrossRef\]](#) [\[PubMed\]](#)
18. Zhang, S.; Wang, S.; Zhang, Q.; Li, Y.; Xing, Y.; Ren, G. Reuse of ammonium sulfate double salt crystals formed during electrolytic manganese production. *Water Sci. Technol.* **2020**, *82*, 615–626. [\[CrossRef\]](#)
19. Gan, Y.; Hang, Z.; Wu, B.; Li, H.; Zhang, W.; Sun, Y.; Li, R.; Zhang, S. Basicity of titanium-based coagulants matters in the treatment of low-turbidity water. *Sep. Purif. Technol.* **2022**, *281*, 119989. [\[CrossRef\]](#)
20. Chen, Y.Z.; Nakazawa, Y.; Matsui, Y.; Shirasaki, N.; Matsushita, T. Sulfate ion in raw water affects performance of high-basicity PACT coagulants produced by Al(OH)(3) dissolution and base-titration: Removal of SPAC particles by coagulation-flocculation, sedimentation, and sand filtration. *Water Res.* **2020**, *183*, 116093. [\[CrossRef\]](#)
21. APHA. *Standard Methods for the Examination of Water and Wastewater*, 20th ed.; American Public Health Association: Washington, DC, USA, 2005.
22. Tang, H.; Stumm, W. The coagulating behaviors of Fe(III) polymeric species—I. Preformed polymers by base addition. *Water Res.* **1987**, *21*, 115–121. [\[CrossRef\]](#)
23. Liu, B.B.; Gao, Y.; Yue, Q.Y.; Guo, K.Y.; Gao, B.Y. The suitability and mechanism of polyaluminum-titanium chloride composite coagulant (PATC) for polystyrene microplastic removal: Structural characterization and theoretical calculation. *Water Res.* **2023**, *232*, 119690. [\[CrossRef\]](#) [\[PubMed\]](#)
24. Guo, K.Y.; Wang, Z.N.; Pan, J.W.; Liu, B.B.; Wang, Y.; Yue, Q.Y.; Gao, Y.; Gao, B.Y. Highly efficient Al-Ti gel as a coagulant for surface water treatment: Insights into the hydrolysate transformation and coagulation mechanism. *Water Res.* **2022**, *221*, 118826. [\[CrossRef\]](#) [\[PubMed\]](#)
25. Cheng, K.; Wang, H.; Li, J.; Li, F. An Effective Method to Remove Antimony in Water by Using Iron-Based Coagulants. *Water* **2020**, *12*, 66. [\[CrossRef\]](#)
26. Lartiges, B.; El Samrani, A.G.; Montarges-Pelletier, E.; Bihannic, I.; Briois, V.; Michot, L. Aggregating ability of ferric chloride in the presence of phosphate ligand. *Water Res.* **2019**, *164*, 114960. [\[CrossRef\]](#)
27. Wang, W.; Qi, L.; Zhang, P.; Luo, J.; Li, J. Removal of COD in wastewater by magnetic coagulant prepared from modified fly ash. *Environ. Sci. Pollut. Res.* **2022**, *29*, 52175–52188. [\[CrossRef\]](#)
28. Yu, H.; Zhang, H.; Sun, Z.; Wang, Y.; Liu, H.; Tong, Y.; Wu, L.; Deng, J.; Sun, L. Effect of polyaluminium silicate sulphate with different alkyl chain lengths on oily sewage in oil fields. *Chem. Eng. J.* **2022**, *450*, 138125. [\[CrossRef\]](#)
29. Wei, Y.; Ding, A.; Chen, Y. Removal of refractory dyes by a novel chlorine-free coagulant of polyferric-silicate-acetate (PFSA): Characterization and performance evaluation. *J. Environ. Chem. Eng.* **2022**, *10*, 108524. [\[CrossRef\]](#)
30. Zhuang, J.; Qi, Y.; Yang, H.; Li, H.; Shi, T. Preparation of polyaluminum zirconium silicate coagulant and its performance in water treatment. *J. Water Process Eng.* **2021**, *41*, 102023. [\[CrossRef\]](#)
31. Zhang, H.; Yu, H.; Deng, J.; Wu, L.; Hu, M.; Tong, Y.; Sun, L.; Liu, H. Preparation of polyaluminium silicate sulphate by gravity supercritical method and its coagulation in oily sewage. *Chemosphere* **2023**, *313*, 137504. [\[CrossRef\]](#)
32. Dayarathne, H.N.P.; Angove, M.J.; Aryal, R.; Abuel-Naga, H.; Mainali, B. Removal of natural organic matter from source water: Review on coagulants, dual coagulation, alternative coagulants, and mechanisms. *J. Water Process Eng.* **2021**, *40*, 101820. [\[CrossRef\]](#)
33. Koul, B.; Bhat, N.; Abubakar, M.; Mishra, M.; Arukha, A.P.; Yadav, D. Application of Natural Coagulants in Water Treatment: A Sustainable Alternative to Chemicals. *Water* **2022**, *14*, 3751. [\[CrossRef\]](#)
34. Liu, H.; Dai, K.; Deng, J.; Zhao, L.; Yu, H.; Zhang, H.; Tong, Y.; Wu, L.; Sun, L. Synthesis of antibacterial polyaluminium silicate sulfate /sepiolitenano composite coagulant for oilfield sewage treatment. *J. Clean. Prod.* **2022**, *379*, 134385. [\[CrossRef\]](#)



35. Yu, L.; Liu, P.; Zheng, K. Preparation of poly-silicate aluminium magnesium zinc (psamz) coagulant and its application for the treatment of oily sludge. *Environ. Eng. Manag. J.* **2022**, *21*, 1557–1567. [[CrossRef](#)]
36. Tang, H.; Xiao, F.; Wang, D. Speciation, stability, and coagulation mechanisms of hydroxyl aluminum clusters formed by PACl and alum: A critical review. *Adv. Colloid Interface Sci.* **2015**, *226*, 78–85. [[CrossRef](#)]

**Disclaimer/Publisher’s Note:** The statements, opinions and data contained in all publications are solely those of the individual author(s) and contributor(s) and not of MDPI and/or the editor(s). MDPI and/or the editor(s) disclaim responsibility for any injury to people or property resulting from any ideas, methods, instructions or products referred to in the content.